NRC·CNRC

NRC Publications Archive
Archives des publications du CNRC

Laser-induced breakdown spectroscopy on aluminum alloy targets

Sabsabi, Mohamad; Cielo, Paolo G.; Boily, Stephane; Chaker, Mohamed

This publication could be one of several versions: author's original, accepted manuscript or the publisher's version. / La version de cette publication peut être l'une des suivantes : la version prépublication de l'auteur, la version acceptée du manuscrit ou la version de l'éditeur.
For the publisher's version, please access the DOI link below./ Pour consulter la version de l'éditeur, utilisez le lien DOI ci-dessous.

Publisher's version / Version de l'éditeur:
https://doi.org/10.1117/12.166288
Optical Methods for Chemical Process Control, SPIE Proceedings, pp. 191-201, 1993-12-31

NRC Publications Archive Record / Notice des Archives des publications du CNRC :
https://nrc-publications.canada.ca/eng/view/object/?id=bc06e80a-9744-4a2e-84ae-c8a777dd15cc
https://publications-cnrc.canada.ca/fra/voir/objet/?id=bc06e80a-9744-4a2e-84ae-c8a777dd15cc

Access and use of this website and the material on it are subject to the Terms and Conditions set forth at
https://nrc-publications.canada.ca/eng/copyright
READ THESE TERMS AND CONDITIONS CAREFULLY BEFORE USING THIS WEBSITE.

L'accès à ce site Web et l'utilisation de son contenu sont assujettis aux conditions présentées dans le site
https://publications-cnrc.canada.ca/fra/droits
LISEZ CES CONDITIONS ATTENTIVEMENT AVANT D'UTILISER CE SITE WEB.

Questions? Contact the NRC Publications Archive team at PublicationsArchive-ArchivesPublications@nrc-cnrc.gc.ca. If you wish to email the authors directly, please see the first page of the publication for their contact information.

Vous avez des questions? Nous pouvons vous aider. Pour communiquer directement avec un auteur, consultez la première page de la revue dans laquelle son article a été publié afin de trouver ses coordonnées. Si vous n'arrivez pas à les repérer, communiquez avec nous à PublicationsArchive-ArchivesPublications@nrc-cnrc.gc.ca.

National Research Council Canada | Conseil national de recherches Canada

Canada

PROCEEDINGS OF SPIE

SPIEDigitalLibrary.org/conference-proceedings-of-spie

Laser-induced breakdown spectroscopy on aluminum alloy targets

Mohamad Sabsabi, Paolo Cielo, Stephane Boily, Mohamed Chaker

Mohamad Sabsabi, Paolo G. Cielo, Stephane Boily, Mohamed Chaker, "Laser-induced breakdown spectroscopy on aluminum alloy targets," Proc. SPIE 2069, Optical Methods for Chemical Process Control, (31 December 1993); doi: 10.1117/12.166288

Event: Optical Tools for Manufacturing and Advanced Automation, 1993, Boston, MA, United States

SPIE.

Downloaded From: https://www.spiedigitallibrary.org/conference-proceedings-of-spie on 31 Aug 2023 Terms of Use: https://www.spiedigitallibrary.org/terms-of-use

LASER-INDUCED BREAKDOWN SPECTROSCOPY ON ALUMINUM ALLOY TARGETS

M. Sabsabi and P. Cielo
National Research Council Canada, Industrial Materials Institute
75 de Mortagne Blvd., Boucherville, Québec J4B 6Y4 CANADA
and
S. Boily and M. Chaker
Institut National de la Recherche Scientifique
1600 Montée Ste-Julie, P.O. Box 1020, Varennes, Québec J0L 2P0 CANADA

ABSTRACT

A laser-induced plasma is used for atomization, ionization and excitation of elements in solid samples. The temporal and spatial behavior of the plasma is studied by observing the emission lines of neutral aluminum and magnesium. The optimal temporal choice was determined for our plasma spectrochemical analysis and a calibration curve for an aluminum-magnesium alloy was obtained.

1. INTRODUCTION

When a high-power pulse is focused on a metal target, the irradiation in the focal spot leads to rapid local heating of the material. For fluxes $\phi > 10^8$ W/cm^2, the material is vaporized and ionized, and a plasma with high temperature and electron density is formed. The plasma characteristics depend on the laser intensity, wavelength, pulse duration, the target material, and also the surrounding atmosphere. In such a medium, neutral and ionized atoms in excited states are present, and spectroscopic analysis of the light emission can be used to determine the composition of the sample. This method is known as "Laser-Induced Breakdown Spectroscopy" (LIBS). The basic features of this technique are described in a few review papers[1-4], while a variety of applications have been reported[5-15].

In terms of aluminum applications, Dhez and Jaegle[16] studied the spectral emission over the 100-200 nm range from plasmas produced by a ruby laser on an Al target in vacuum. McMordie and Roberts[17] modeled the interaction of pulsed CO_2 laser radiation with aluminum, again in vacuum. Rosen et al[18] presented results for the thermal and mechanical coupling of pulsed UV laser energy to aluminum targets (Al2024) irradiated in a vacuum using an XeF laser ($\lambda \approx 0{,}35$ µm, pulse duration ≈ 1 µs). Rothenberg and Koren[19] performed a comparative study of the laser produced plasma in a vacuum at the surface of transparent crystalline α - Al_2O_3 (sapphire) and Al metal using 248-nm excimer laser pulses (15 ns) and explained the relative threshold intensity for plasma production in these two cases. A detailed study of ultraviolet and visible spectroscopy of Al plasmas has been carried out by Knudtson et al[20] using 2 µs pulses from a flashlamp-pumped dye laser operated using Rh6G dye at 583 nm. Tambay et al[21] studied the laser produced Al plasma in vacuum using Nd:YAG laser radiation and its second, third and fourth harmonics. They studied the spatial variation of temperature and electron density along the axis of expansion of the plasma.

As to laser produced Al plasma in air at atmospheric pressure, Scott and Strasheim[22] found that the background is more intense in the case of a Q-switched laser-induced plasma than in the plasma induced by longer laser pulses. The time profiles of the Al(I), Al(II), and Al(III) lines reached their maximum intensities at 1.2, 0.9 and 0.2 µs, respectively. Temporally resolved spectrometric observations of laser-produced aluminum alloy plasmas have been reported by Piepemeier and Malmstadt[23] and Adrain et al[24]. The emission spectra of species evaporated by a laser pulse (10.6 µm, 25 µs, up to 18 J) from an alumina surface in air has been analyzed by Wei et al[25] and Wei[26]. Golub and Nemchinov[27] evaluated numerically the early behavior of plasma in air above an aluminum target irradiated with neodymium or CO_2 laser pulses. It follows from their calculations that the threshold for plasma formation is not greatly affected by changing the laser radiation wavelength from 1.06 to 10.6 µm. Optical spectroscopy of a plasma produced by focusing CO_2 laser radiation (10.6 µm, 1.8 µs, 50 J) on an aluminum target in air has been reported by McKay et al[28]. Plasma electron temperatures of the order of 12000 K for aluminum and 16000 K for nitrogen were evaluated[28]. Poprawe et al[29] observed the spectra of

0-8194-1334-8/93/$6.00

Downloaded From: https://www.spiedigitallibrary.org/conference-proceedings-of-spie on 31 Aug 2023
Terms of Use: https://www.spiedigitallibrary.org/terms-of-use

aluminum and copper plasmas induced in air and vacuum by a KrF-excimer laser. Sokolowski et al[30] presented the results of spectral diagnostics of the plasma produced by the intense CO_2 laser during the welding process of steel and aluminum. More recently, Ownes and Majidi[31] described the optimization of the buffer gas and its pressure to improve the signal-to-background ratio on LIBS. They observed a maximum emission intensity for the aluminum ionic transition at 281.6 nm when helium was employed as the buffer gas.

In the present work we examined the time-resolved spectra of laser-induced plasmas on aluminum alloys. We determined the optimum period over the plasma lifetime for spectral chemical analysis of a magnesium-aluminum alloy, and we established a calibration curve for such an alloy.

2. DESCRIPTION OF THE EXPERIMENTAL SETUP

The experimental arrangement is illustrated in Fig. 1. A pulsed KrF excimer laser (Hyper 400, Lumonics) was used for solid ablation at the wavelength of 248 nm. The laser was focused by a simple lens L_1 (f_1 = 1 m) through the quartz window of the chamber onto the surface of the sample at 45° incidence. The radiation of the laser produced plasma was observed at 135° to the laser beam using two imaging quartz lenses L_1 and L_2, a plane grating spectrograph and a photomultiplier as detector.

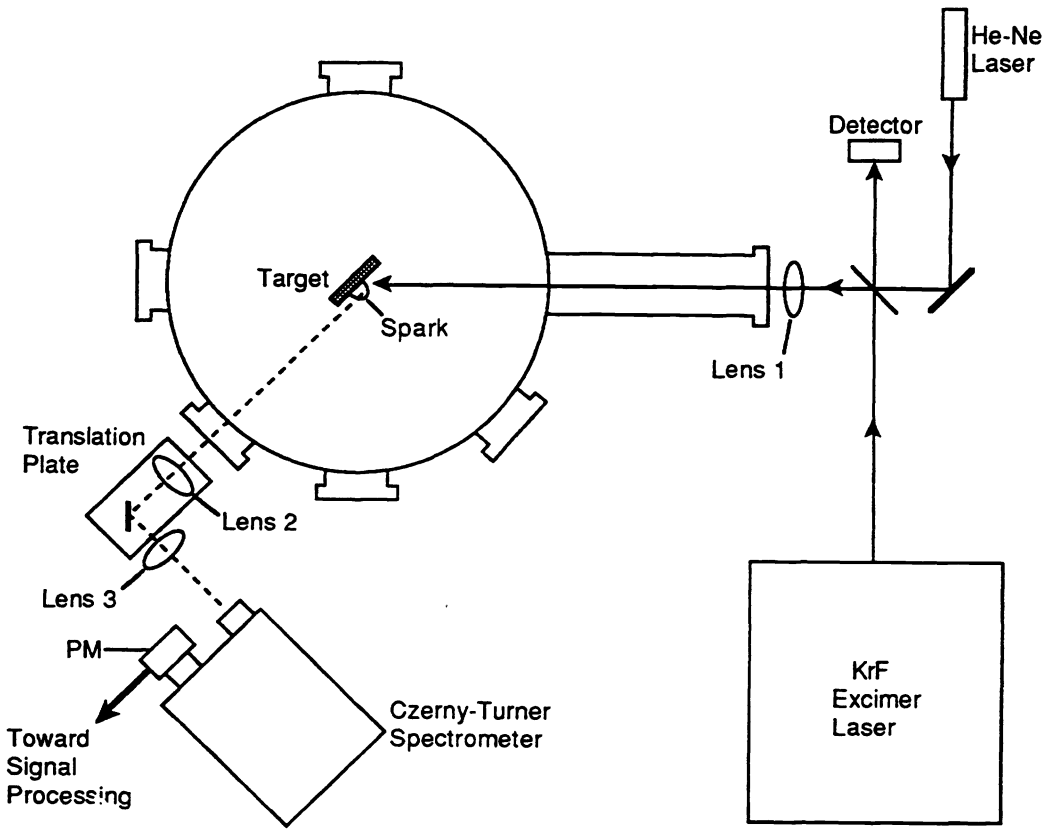

Fig. 1. Schematic diagram of the experimental apparatus (not to scale).

Downloaded From: https://www.spiedigitallibrary.org/conference-proceedings-of-spie on 31 Aug 2023
Terms of Use: https://www.spiedigitallibrary.org/terms-of-use

The laser energy was 100 mJ/pulse with a pulse duration (nominal FWHM) of 12 ns. The maximum repetition rate was 20 shots per second, but for most measurements a rate of only one shot/second was used (1 Hz). The relative standard deviation of the pulse energy measured with a calibrated calorimeter was typically 6%. We added fluorine gas within the laser cavity during the experiment to keep a high efficiency for the ArF mixture and avoid a decrease of laser energy with time.

The samples were placed in a cylindrical vacuum-tight chamber (1 m^3), which could be evacuated by a pump system. The sample was rotated between pulses in order to expose a fresh surface to each laser pulse. Space-resolved studies of LIBS were carried out by translating the optical axis (by moving the translation plate in increments of 0.5 mm). The sample surface was parallel to the spectrometer sight line, so that transverse movement of the translation plate enabled us to collect the plasma emission at a particular distance from the sample surface to be analyzed. The plasma was imaged 3:1 by a quartz lens (L_2, f_2 = 30 cm; L_3, f_3 = 1m, beam collimated between the two lenses) onto the entrance 0.1 mm-wide slit of a Czerny-Turner spectrograph which had a grating with 1200 grooves/mm blazed at 500 nm, and reciprocal linear dispersion of 0.80 nm/mm.

A high-sensitivity photomultiplier tube (RCA IP28) was used as the detector. The overall response time was of about 2 ns. The photomultiplier signal was displayed on a 250 MHz digital oscilloscope (Phillips PM3320A) and the digitized wave for data could be transferred to the computer for storage and analysis. All signals used in the plots and calculations were background corrected and normalized with the spectral response of the system (Lenses + Spectrometer + PM). The wavelengths of the obtained spectra were calibrated using a Hg(Ar) spectral calibration lamp. The calibration response of the system was carried out using a Labsphere Unisource 1200 lamp.

3. EXPERIMENTAL RESULTS AND DISCUSSION

3.1 Spectral analysis of the plasma emission and signal conditioning

The spectral distribution of the plasma emission in the near-UV and visible range was analyzed using sequential laser shots to scan the full spectrum. Figure 2 shows a spectrum emitted by the laser induced plasma on an aluminum alloy at atmospheric pressure.

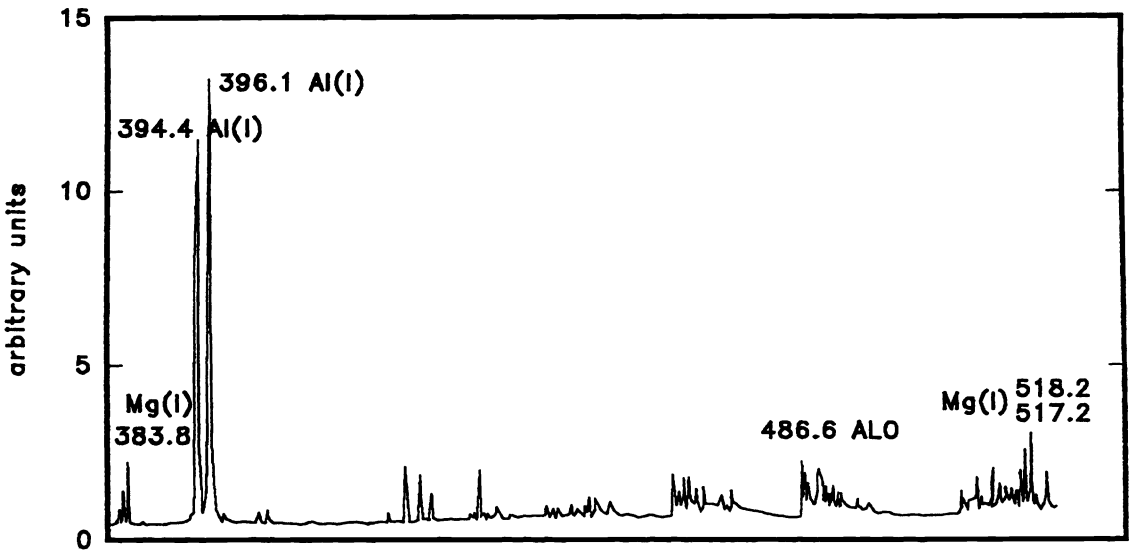

Fig. 2. Spectrum emitted by a laser-induced plasma on an aluminum alloy Al6061 target, pointing distance z=1.5 mm from the target surface, laser intensity 1.5E+9 W/cm^2, in air at the atmospheric pressure.

Downloaded From: https://www.spiedigitallibrary.org/conference-proceedings-of-spie on 31 Aug 2023
Terms of Use: https://www.spiedigitallibrary.org/terms-of-use

In this spectrum we identified a few lines of atomic and ionic aluminum, molecular bands of AlO, and emission lines of magnesium. Table I lists the parameters of a few atomic emission lines of interest for a relative analysis of aluminum and magnesium in the plasma.

TABLE I

TRANSITION	λ, Mg (nm)	E_1 (eV)	E_2 (eV)	A_{21} (s^{-1})	g_2
$3p^0P^0 - 3d\ ^3D$	3838	2.72	5.95	$1.68.10^8$	7
$3p^1P^0 - 5d\ ^1D$	4902	4.35	6.98	$0.16.10^8$	5
$3p^3P^0 - 4s\ ^3S$	5183	2.72	5.11	$0.575.10^8$	3
$3d^2D^0 - 4p\ ^2P$	5528	4.35	6.59	$0.14.10^8$	5
	λ, Al				
$3p^2P^0 - 3d\ ^2D$	3082	0,00	4.02	$0.61.10^8$	4
$3p^2P^0 - 4s\ ^2S$	3961	0,01	3.14	$0.98.10^8$	2

Source Tables N.B.S. [32]

The observed background continuum is due mainly to free-free and free-bound transitions in air, as well as to broadened atomic lines and molecular bands. Note that these spectra are obtained by integrating, for each spectral position, the emitted intensity over the total time of excitation and decay of the plasma. The air pressure is a crucial parameter in this mutual diffusion process. It determines the mean free path of the particles, which affects the atomization, excitation and ionization processes. As discussed by several authors[5, 15, 31], the surrounding atmosphere affects the emission spectra, the crater size and the amount of sample vaporized by the laser pulse.

The line-to-background (L/B) ratio is an important factor in LIBS spectro-chemical analysis. It is known that the precision and spectral detection limit are dependent on the value of this ratio. A large value in the L/B ratio can be achieved either by decreasing the background emission or by increasing the line intensity. Figure 3 shows profiles of the Mg(I) 383.8 nm emission (line + continuum) and the nearby background region at 384.8 nm in order to compare the behavior of an emission line and the continuum. The background intensity decays much faster than the line intensity. The line-to-background ratio (L/B) therefore increases with time (Figure 4) up to about 2 μs, at which time the background signal has decayed to practically zero . This behavior is typical of most atomic lines.

The L/B ratios of the spectra were also found to be time and position dependent in the plasma. The region near the metal surface is energetic enough to be a strongly luminous plasma, which emits an undesirable spectral continuum background. Furthermore, the plasma is very hot during the first microsecond after the laser pulse. The continuum is preferentially excited near the surface, whereas the spectral lines extend much further. Because the continuum background is very low in the outer plasma region, it is possible to improve the L/B ratio by choosing an appropriate region at appropriate times, as will be discussed below.

Downloaded From: https://www.spiedigitallibrary.org/conference-proceedings-of-spie on 31 Aug 2023
Terms of Use: https://www.spiedigitallibrary.org/terms-of-use

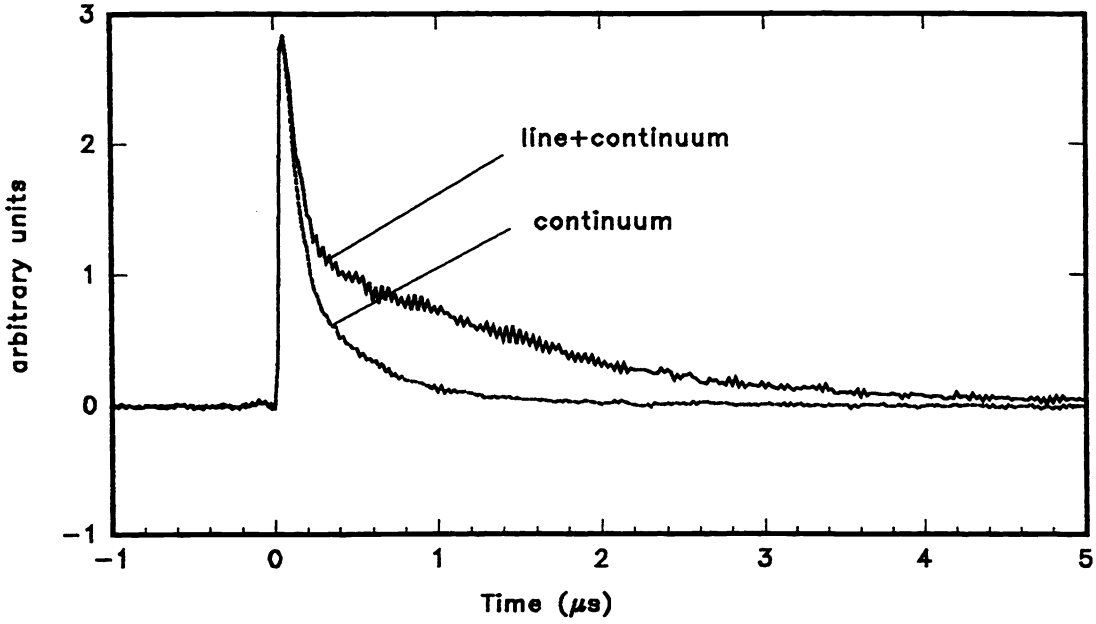

Fig. 3. Temporal emission signals from laser induced plasma at 383.8 nm {Mg(I) line + continuum} and 384.8 nm {continuum only}. z=0.5 mm, target Al6061, 1.5E+9 W/cm^2.

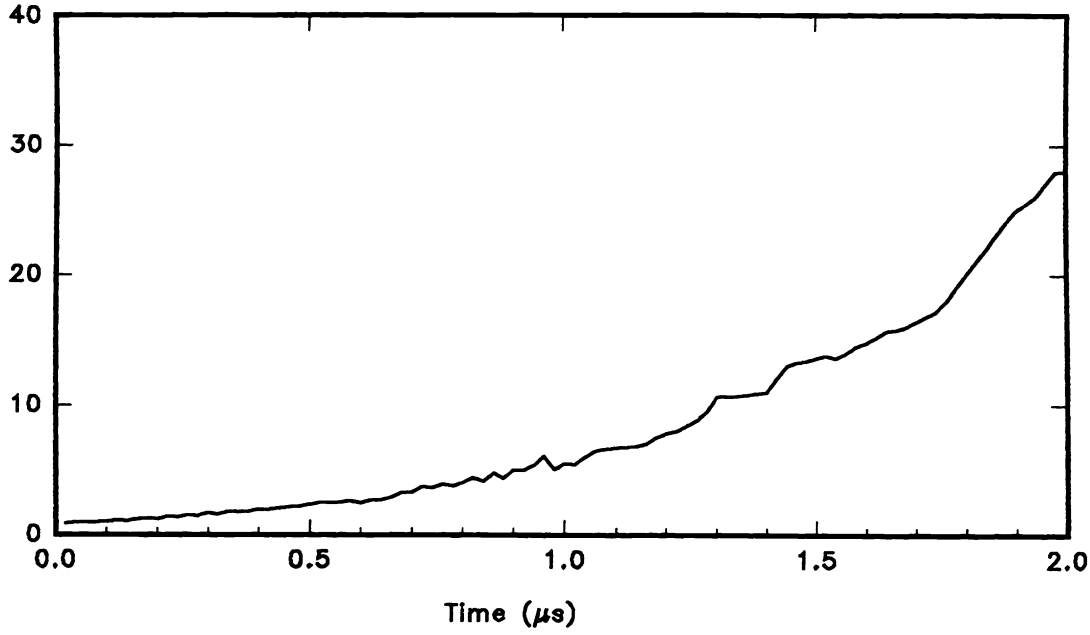

Fig. 4. Ratio of the above 383.8 and 384.8 emission lines.

Downloaded From: https://www.spiedigitallibrary.org/conference-proceedings-of-spie on 31 Aug 2023
Terms of Use: https://www.spiedigitallibrary.org/terms-of-use

3.2 Intensity Measurements and Elemental Analysis

There are two main factors influencing the emitted line intensities: the first is the number density of the atoms, and the second is the temperature of the plasma. The quantitative spectral analysis involves relating the spectral line intensity of an element in the plasma to the concentration of that element in the target. The emitted spectral line intensity is a measure of the population of a given energy level in the plasma, which is then assumed to be a reliable indicator of the sample composition.

We investigated a set of seven samples (Al6061, Al5182, as well as five home-made binary Mg-Al samples) with widely varying magnesium concentrations (see Table II).

TABLE II

SAMPLES	Mg	Al
AL6061	1%	97.9
AL5182	4.6%	95.2
# 1	8%	91.9
# 2	12%	87.8
# 3	16%	83.9
# 4	20%	79.8
Mg pure	99.99%	0

The results in Figure 5 show the 383.8 nm emission signal versus time of Mg(I) for different concentrations, always with the background subtracted. This variation shows the basic capability of LIBS to establish a correlation between the observed integrated signal and the amount of a given element in the target. It will be observed, however, that the initial portion of the emitted signals is often perturbed, possibly because of background fluctuations or of selective vaporization problems, as will be discussed below. Also, for a more reliable elemental analysis the Mg emission should be ratioed against a reference emission from the most abundant component, typically Al, to compensate for plasma temperature variations.

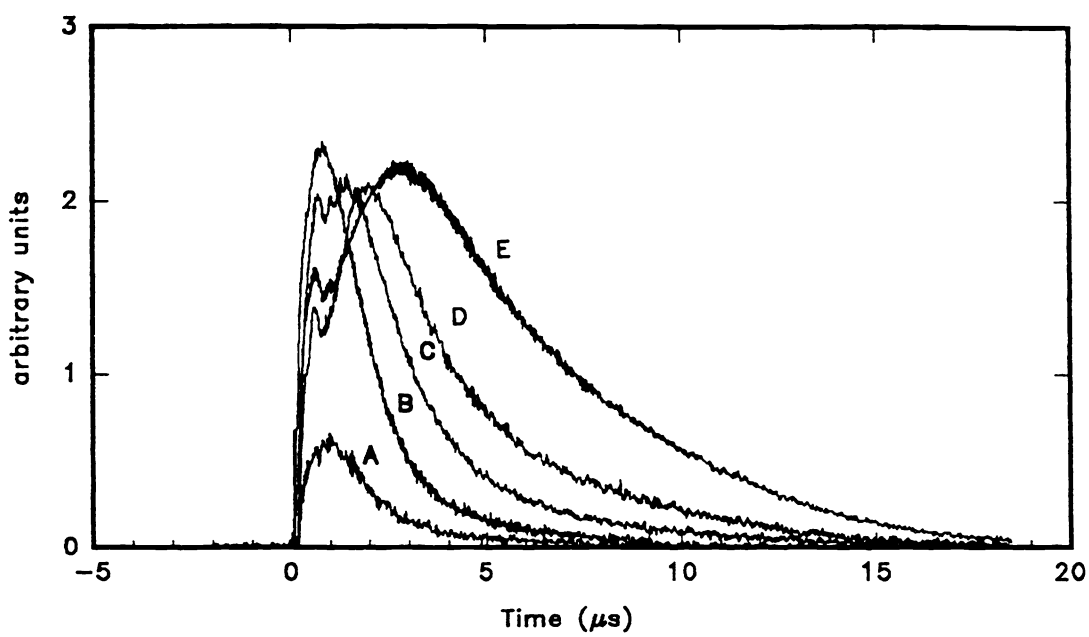

Fig. 5. Emission signals from the 383.8 nm Mg line for a number of samples having different Mg contents (A: 1%, B: 8%, C: 12%, D: 16%, and E: 20% of Mg in Al). z=0.5 mm, 1.5E+9 W/cm^2 in air at atmospheric pressure.

Downloaded From: https://www.spiedigitallibrary.org/conference-proceedings-of-spie on 31 Aug 2023
Terms of Use: https://www.spiedigitallibrary.org/terms-of-use

Figure 6 shows the measured intensities, in arbitrary units, of the 383.8 nm Mg and 396.1 nm Al lines versus time for a 12% weight concentration of Mg in Al. The Mg line reached the maximum intensity at about 1.5 μs, while the Al line peaked at about 2.5 μs. This different temporal behavior may be due to the lower vaporization temperature of Mg (1107°C) as compared to Al (2450°C). This can produce selective evaporation effects[33] in the molten material in thermal contact with the plasma. Such effects tend to be less important in the latter portion of the emission signal, when atomization of eventual ejected particles is completed and thermal exchanges are much reduced.

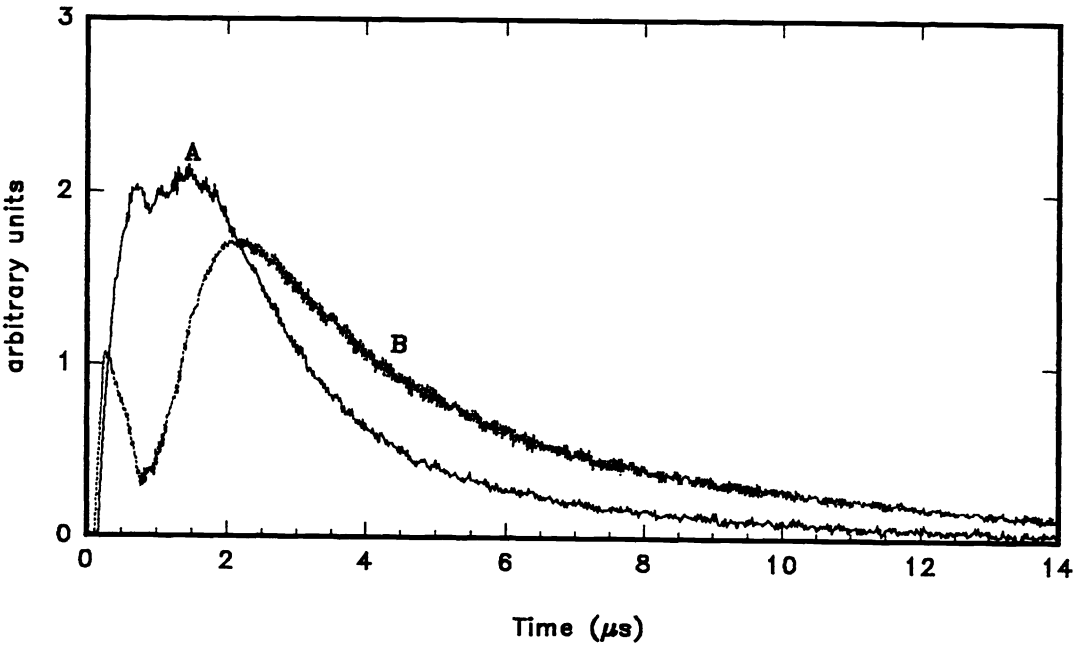

Fig. 6. Emission signals from the Mg 383.8 nm (A) and the Al 396.1 nm (B) lines, as obtained for a 12% Mg sample at the conditions above.

The spatial distribution of the laser-induced plasma in the direction normal to the sample surface could be investigated by moving the translation plate shown in Figure 1. It was found that the plasma emission signals evoluate interdependently in terms of time, space and choice of the emission line. Figure 7 shows the intensity ratio I_{Mg}/I_{Al} for several positions above the sample. The ratio decreases within the first 2 μs, but becomes almost constant within the experimental uncertainty for times larger than 3 μs.

Figure 8 plots the values of the same intensity ratio I_{Mg}/I_{Al} as measured at different times in different samples against the concentration ratio C_{Mg}/C_{Al} within these samples. There is a quasi-linear dependence of I_{Mg}/I_{Al} on C_{Mg}/C_{Al} within the experimental uncertainty. The scattering of the experimental data is believed to be mainly due to sample inhomogeneity as well as to shot-to-shot plasma variability. Self-absorption for the Al 396.1 nm line should not significantly affect the calibration linearity within the limited relative variation of the Al concentration, while the 383.8 nm Mg line is nonresonant and thus optically thin.

CONCLUSION

The laser-induced plasma in a number of aluminum-magnesium alloys has been investigated for different concentrations of magnesium. We found that the best time interval for spectral analysis was between 3 and 5 μs of the plasma lifetime, i.e., a gate of 2 μs with delay time of 3 μs. By avoiding the early 3 μs of the signal, one can avoid the strong backround continuum, minimize partial atomization and selective evaporation problems, and better resolve the narrower emission lines. On the other hand, we found it preferable to eliminate the signal portion exceeding 5 μs, where the emission intensity becomes too low to substantially improve the signal/noise ratio.

Downloaded From: https://www.spiedigitallibrary.org/conference-proceedings-of-spie on 31 Aug 2023
Terms of Use: https://www.spiedigitallibrary.org/terms-of-use

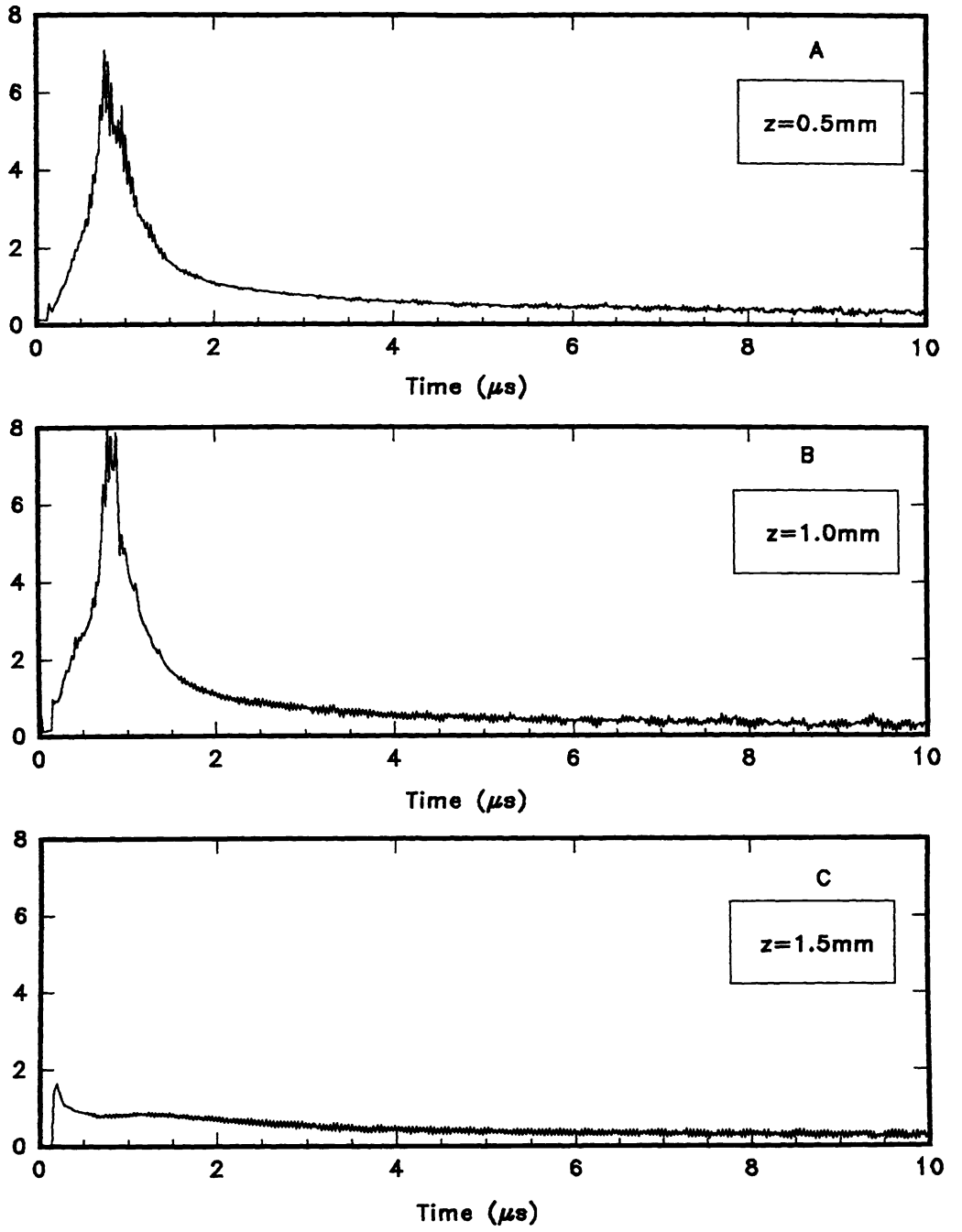

Fig. 7. Temporal evolutions of the ratio of the 383.8 nm Mg line and the 396.1 nm Al line as obtained when pointing at different distances z from the target surface, laser intensity 1.5E+9 W/cm^2, in air at the atmospheric pressure.

Downloaded From: https://www.spiedigitallibrary.org/conference-proceedings-of-spie on 31 Aug 2023
Terms of Use: https://www.spiedigitallibrary.org/terms-of-use

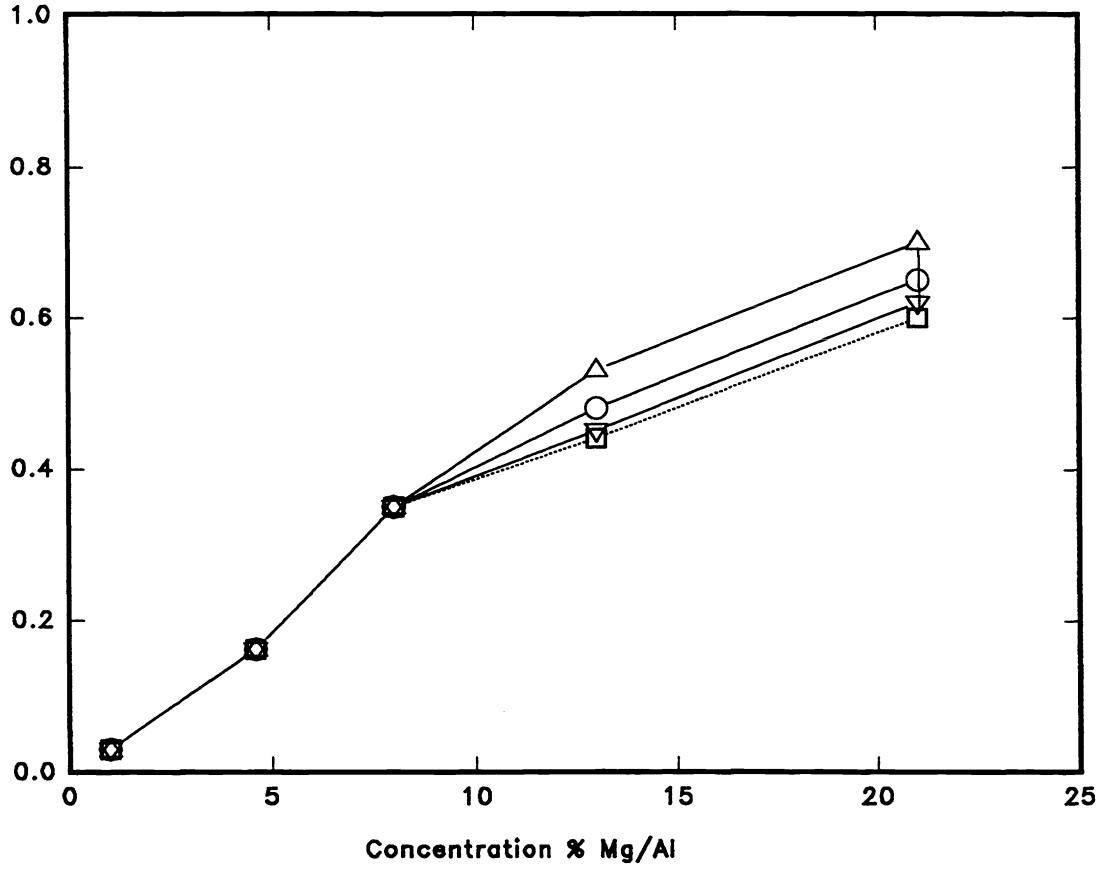

Fig. 8. Calibration curves obtained for the Mg-Al samples, z=1.5 mm, for different delay times: 3 μs (up-triangles), 4 μs (circles), 5 μs (down-triangles) and 6 μs (squares).

REFERENCES

1) R.S. Adrain and J. Watson, "Laser microspectral analysis: a review of principles and applications" J. Phys. D: Appl. Phys., **17**, 1915 (1984).

2) L.J. Radziemski and D.A. Cremers, "Laser-induced Plasmas and Applications". M. Dekker, New York, 1989.

3) L. Moenke-Blankenburg, "Laser Microanalysis". J. Wiley & Sons, New York, 1989.

4) V. Majidi and M.R. Joseph "Spectroscopic Applications of laser-induced plasmas", Critical Review in Anal. Chem., **23**, 143 (1992).

5) J.B. Ko, W. Sdorra and K Niemax, "Basic investigations for laser microanalysis: III Application of different buffer gases for laser-produced sample planes" Mikrochim. Acta, **107**, 319 (1992).

6) F. Leis, W. Sdorra, J.B. Ko and K. Niemax, "Basic investigations for laser microanalysis: I. Optical emission spectrometry of laser-produced sample plumes" Mikrochim. Acta, **2**, 185 (1989).

Downloaded From: https://www.spiedigitallibrary.org/conference-proceedings-of-spie on 31 Aug 2023
Terms of Use: https://www.spiedigitallibrary.org/terms-of-use

7) T. Ozaki, T. Takahashi, Y. Iwai, K. Gunji and E. Sudo, "Giant pulse laser direct spectrochemical analysis of C, Si and Mn in liquid iron" Trans. ISIJ, **23**, 463 (1983).

8) C.J. Lorenzen, C. Carlhoff, U. Hahn and M. Jogwich, "Applications of laser-induced emission spectral analysis for industrial process and quality control" J. Anal. Atom. Spectr., **7**, 1029 (1992).

9) D.A. Cremers, "The analysis of metals at a distance using laser-induced breakdown spectroscopy", Appl. Spectrosc., **41**, 572 (1987).

10) K.J. Grant, G. L. Paul, J. O'Neill, "Quantitative elemental analysis of iron ore by laser-induced breakdown spectroscopy, Appl. Spectrosc., **45**, 701 (1991).

11) D. Franzke, H. Klow, A. Wokaun, "Element identification on the surface of inorganic solids by excimer laser-induced emission spectroscopy, Appl. Spectrosc., **46**, 587 (1992)

12) D.K. Ottesen, "Detection of contaminants on electronic microcircuit substrates by laser spark emission spectroscopy", Appl. Spectrosc., **46**, 593 (1992).

13) C. Aragon, J.A. Aguilera and J. Campos, "Determination of carbon content in molten steel using laser-induced breakdown spectroscopy", J. Appl. Spectrosc., **47**, 606 (1993).

14) Y. I. Lee, S.P. Sawan, T.L. Thiem, Y.Y. Teng, J. Sneddon, "Interaction of a laser beam with metals. Part II: Space-resolved studies of laser-ablated plasma emission", Appl. Spectrosc., **46**, 436 (1992).

15) Y.I. Lee, T.L. Theim, G.H. Kim, Y.Y. Teng and J. Sneddon, "Interaction of an excimer laser beam with metals. Part III: The effect of a controlled atmosphere in laser ablated plasma emission", Appl. Spectrosc., **46**, 1599 (1992).

16) P. Dhez, P. Jaegle, S. Leach and M. Velghe, "Some characteristics of the extreme UV spectrum emitted by the plasma produced by laser impact on an aluminum target" J. Appl. Phys., **40**, 2545 (1969).

17) J.A. McMordie and P.P. Roberts, "The interaction of pulsed CO_2 laser radiation with aluminum", J. Phys. D: Appl. Phys., **8**, 768 (1975).

18) D.I. Rosen, J. Mitteldorf, G. Kothandaram, A.N. Pirri, and E.R. Pugh, "Coupling of pulsed 0,35 μm laser radiation to aluminum alloys", J. App. Phys., **53**, 3190 (1982).

19) J. Rothenberg and G. Koren, "Laser produced plasma in crystalline α-Al_2O_3 and aluminum metal", Appl Phys. Lett., **44**, 664 (1984).

20) J.T. Knudtson, W.B. Green and D.G. Sutton, "The UV-visible spectroscopy of laser-produced plasmas" J. Appl. Phys., **61**, 4771 (1987).

21) R. Tambay, R. Singh and R.K. Thareja, "Studies on recombining Al-plasma using 1.06, 0.532, 0.355 and 0.266 μm laser radiation" J. Appl. Phys., **72**, 1197 (1992).

22) R.H. Scott, A. Strasheim, "Laser induced plasma for analytical spectroscopy", Spectrochim. Acta, **25B**, 311 (1970).

23) E.H. Piepmeier, and H.V. Malmsladt, "Q-switched laser energy absorption in the plasma of an aluminum alloy", Anal. Chem., **41**, 700 (1969).

24) R.S. Adrain, J. Watson, P.H. Richards, and A. Maitland, "Laser microspectral analysis of steels", Optics Laser Tech., **2**, 137 (1980).

25) P.S.P. Wei, K.T. Tang, and J.R.B. Hall, "Forbidden transitions in the emission spectrum of atomic aluminum", J. Chem. Phys., **61**, 3593 (1974).

Downloaded From: https://www.spiedigitallibrary.org/conference-proceedings-of-spie on 31 Aug 2023
Terms of Use: https://www.spiedigitallibrary.org/terms-of-use

26) P.S.P. Wei, "Emission spectrum of aluminum in a laser-produced plasma" J. Chem. Phys., **64**, 1531 (1976).

27) A.P. Golub and I.V. Nemchinov, "Time of appearance of a plasma due to action of laser radiation of different wavelengths on an aluminum target in air", Sov. J. Quantum, Electron., **10**, 1058 (1980).

28) J.A. McKay, R.D. Bleach, D.J. Nagel, and J.T. Schriempf, "Pulsed-CO_2-laser interaction with aluminum in air: Thermal response and plasma characteristics", J. App. Phys., **50**, 3231 (1979).

29) R.Poprawe, M. Wehmer, G. Brown, and G. Herziger, "Plasma-spectra in materials processing by excimer Lasers", SPIE, Proceedings of High Power Lasers, **801**, 191 (1987).

30) W. Sokolowski, G. Herziger, and E. Beyer, "Spectroscopic study of laser-induced plasma in the welding process of steel and aluminum", SPIE, Proceedings of High Power Lasers and Laser Machining Technology, **1132**, 288 (1989).

31) M. Ownes and V. Majidi, "Effects of high pressure buffer gases on emission from laser-induced plasmas", Appl. Spectrosc., **45**, 1463 (1991).

32) J. Reader, C. H. Corliss, W.L. Wiese, and O.A. Martin, "Wavelength and Transition Probabilities for Atoms and Atomic Ions", National Standard Reference Data System-NBS68 (US Government Printing Office, Washington DC, 1980); W.L. Wiese, M.W. Smith, and B.M. Miles, "Atomic Transition Probabilities", Vol. II Sodium through Calcium CA Critical Data Compilation, National Standard Reference Data System-NBS22 (US Government Printing Office, Washington, DC, 1969).

33) J.B. Ko, W. Sdorra and K. Niemax, "On the internal standardization in optical emission spectrometry of the plasmas produced by laser ablation of solid samples" Fresenius Z. Anal. Chem., **335**, 648 (1989).

Downloaded From: https://www.spiedigitallibrary.org/conference-proceedings-of-spie on 31 Aug 2023
Terms of Use: https://www.spiedigitallibrary.org/terms-of-use